The Journal of Immunology

Identification of Multiple Isolated Lymphoid Follicles on the Antimesenteric Wall of the Mouse Small Intestine

Hiromasa Hamada, Takachika Hiroi, Yasuhiro Nishiyama, Hidemi Takahashi, Yohei Masunaga, Satoshi Hachimura, Shuichi Kaminogawa, Hiromi Takahashi-Iwanaga, Toshihiko Iwanaga, Hiroshi Kiyono, Hiroshi Yamamoto and Hiromichi Ishikawa

J Immunol 2002; 168:57-64; ;
doi: 10.4049/jimmunol.168.1.57
http://www.jimmunol.org/content/168/1/57

The Journal of Immunology is published twice each month by
The American Association of Immunologists, Inc.,
1451 Rockville Pike, Suite 650, Rockville, MD 20852

Print ISSN: 0022-1767 Online ISSN: 1550-6606.

Identification of Multiple Isolated Lymphoid Follicles on the Antimesenteric Wall of the Mouse Small Intestine[1]

Hiromasa Hamada,*† Takachika Hiroi,‡ Yasuhiro Nishiyama,*§ Hidemi Takahashi,§ Yohei Masunaga,¶ Satoshi Hachimura,¶ Shuichi Kaminogawa,¶ Hiromi Takahashi-Iwanaga,‖ Toshihiko Iwanaga,# Hiroshi Kiyono,‡ Hiroshi Yamamoto,† and Hiromichi Ishikawa*[2]

We have revealed that 100–200 clusters, filled with closely packed lymphocytes, can be found throughout the length of the antimesenteric wall of the mouse small intestine. They are composed of a large B cell area, including a germinal center, and epithelia overlying the clusters contain M cells. A large fraction of B cells displays $B220^+CD19^+CD23^+IgM^{low}IgD^{high}CD5^-Mac\text{-}1^-$ phenotype, and the composition of IgA^+ B cells is smaller but substantial. To our knowledge, these clusters are the first identification of isolated lymphoid follicles (ILF) in mouse small intestine. ILF can be first detected at 7 (BALB/c mice) and 25 (C57BL/6 mice) days after birth, and lymphoid clusters equivalent in terms of cellular mass to ILF are present in germfree, athymic nude, *RAG-2*$^{-/-}$, TCR-$\beta^{-/-}$, and Ig μ-chain mutant ($\mu m^{-/-}$) mice, although c-*kit*$^+$ cells outnumber $B220^+$ cells in germfree and athymic nude mice, and most lymphoid residents are c-*kit*$^+B220^-$ in *RAG-2*$^{-/-}$, TCR-$\beta^{-/-}$, and $\mu m^{-/-}$ mice. ILF develop normally in the progeny of transplacentally manipulated Peyer's patch (PP)-deficient mice, and decreased numbers of conspicuously atrophied ILF are present in IL-7R$\alpha^{-/-}$ PP^{null} mice. Neither ILF nor PP are detectable in lymphotoxin $\alpha^{-/-}$ and *aly/aly* mice that retain well-developed cryptopatches (CP) and thymus-independent subsets of intraepithelial T cells, whereas ILF, PP, CP, and thymus-independent subsets of intraepithelial T cells disappear from common cytokine receptor γ-chain mutant mice. These findings indicate that ILF, PP, and CP constitute three distinct organized gut-associated lymphoid tissues that reside in the lamina propria of the mouse small intestine. *The Journal of Immunology,* **2002, 168: 57–64.**

In the small intestine of mammals, gut-associated lymphoid tissues (GALT)[3] consist of organized lymphoid structures and diffusely distributed populations of cells. Organized GALT are principally comprised of aggregated lymphoid follicles (Peyer's patches; PP) and mesenteric lymph nodes (MLN).

It is now clear that IgA is one of the key hallmarks of the intestinal humoral immune system (1–3) and that PP are the major inductive sites for initiation of Ag-specific IgA responses to a variety of intestinal luminal Ags (4, 5). However, it has been reported that PP are not of paramount importance for establishing strong local IgA Ab responses to foreign protein Ag in rats (6) and to live locally invasive bacteria in rabbit (7). Consistent with these earlier observations, we (8) have recently demonstrated that PP also are not a strict requirement in mice for induction of Ag-specific intestinal IgA Ab responses. Oral immunization of the progeny of mice treated with lymphotoxin β receptor (LTβR) and Ig chimeric protein (LTβR-Ig) that lacked PP but retained MLN (9) with OVA plus cholera toxin as mucosal adjuvant resulted in OVA-specific intestinal IgA Ab responses (8). In contrast, TNF and lymphotoxin (LT) α double-knockout mice that lacked both PP and MLN (10) failed to elicit the responses (8). On the basis of these findings, we underscored the compensatory role of MLN for the induction of mucosal immune responses in LTβR-Ig-treated PP^{null} mice.

Other forms of lymphoid aggregations that have been identified in the wall of human (11), rabbit (7), and guinea pig (12) small intestines are isolated lymphoid follicles (ILF) which are invisible from the serosal or mucosal surface of the small intestine. ILF are structurally and functionally similar to the follicular units that compose PP and are believed to be an equivalent or complementary system to PP for the induction of intestinal IgA Ab responses. In contrast to ILF identified in the above mammals, however, ILF in the mouse small intestine have not been described in the immunological literature to date. Recently, we revealed multiple tiny clusters filled with c-*kit*$^+$IL-7R$^+$Thy-1$^+$ lymphohemopoietic progenitors in crypt lamina propria (LP) of the mouse small intestine (cryptopatches; CP) (13–16) and verified that CP were extrathymic anatomical sites indispensable for intestinal T lymphopoiesis (14–16). The modified nonclassical villi occupied mostly by immature lymphocytes (lymphocyte-filled villi; LFV) have also been identified in the rat small intestine and are regarded as candidates for specialized sites of primary extrathymic T lymphopoiesis (17). In this context, such a continued description of novel GALT is

*Department of Microbiology, Keio University School of Medicine, Tokyo, Japan; †Department of Immunology, Graduate School of Pharmaceutical Science, and ‡Department of Mucosal Immunology, Research Institute for Microbial Diseases, Osaka University, Osaka, Japan; §Department of Microbiology, Nippon Medical School, Tokyo, Japan; ¶Department of Applied Biological Chemistry, University of Tokyo, Tokyo, Japan; ‖Department of Anatomy, School of Medicine, and #Laboratory of Anatomy, Graduate School of Veterinary Medicine, Hokkaido University, Sapporo, Japan

Received for publication August 27, 2001. Accepted for publication October 30, 2001.

The costs of publication of this article were defrayed in part by the payment of page charges. This article must therefore be hereby marked *advertisement* in accordance with 18 U.S.C. Section 1734 solely to indicate this fact.

[1] This work was supported by a Grant-in-Aid for Creative Scientific Research, Ministry of Education, Science, Sports and Culture of Japan; by the Agency of Science and Technology, Japan; by the Japan Society for the Promotion of Science (JSPS-RFTF 97L00701); and by a Keio Gijuku Academic Development Funds.

[2] Address correspondence and reprint requests to Dr. Hiromichi Ishikawa, Department of Microbiology, Keio University School of Medicine, 35 Shinanomachi, Shinjuku-ku, Tokyo 160-8582, Japan. E-mail address: ishikawa@microb.med.keio.ac.jp

[3] Abbreviations used in this paper: GALT, gut-associated lymphoid tissues; *aly*, alymphoplasia; BrdU, bromodeoxyuridine; CP, cryptopatches; CRγ, common cytokine receptor γ-chain; GC, germinal center; GF, germfree; ILF, isolated lymphoid follicles; IEL, intestinal intraepithelial T cells; LFV, lymphocyte-filled villi; LP, lamina propria; LT, lymphotoxin; LTβR, lymphotoxin β receptor; M cells, microfold cells; MLN, mesenteric lymph nodes; μm, Ig μ-chain membrane exon; *nu/nu*, athymic nude; PEC, peritoneal cavity; PI, propidium iodide; PNA, peanut agglutinin; PP, Peyer's patches; *RAG*, recombination-activating gene.

0022-1767/02/$02.00

viewed as a good indication of the complexity of the intestinal immune system that has been driven by millennia of evolutionary pressures (18).

Thus, the continued identification of new organized GALT and a consideration of the reasoning behind this, in conjunction with the significance of our novel findings from LTβR-Ig-treated PP^{null} mice (8), led us to investigate whether lymphoid aggregations equivalent in all respects to ILF are present in the small intestine of laboratory mice. We found that 100–200 lymphoid aggregations that fulfilled the criteria of ILF were aligned along the antimesenteric wall of the mucosa. In the present paper, anatomical structure, organogenesis, lymphocyte composition, and strain-to-strain variation of these newly identified ILF are described in relation to those of the other organized GALT of the mouse small intestine.

Materials and Methods

Mice

BALB/cA/Jcl (B/c), C57BL/6J/Jcl (B6), DBA/2J/Jcl, C3H/HeN/Jcl, athymic nude (*nu/nu*) BALB/cA/Jcl, and alymphoplasia (*aly*) mutant *aly/aly* Jcl (19) mice were purchased from CLEA Japan (Tokyo, Japan). LTα mutant C57BL/6J ($LT\alpha^{-/-}$) mice (20) were purchased from The Jackson Laboratory (Bar Harbor, ME). IL-7R α-chain-deficient ($IL\text{-}7R\alpha^{-/-}$) mice (21), TCR-Cβ mutant ($TCR\text{-}\beta^{-/-}$) mice (22), male mice carrying a truncated mutation of common cytokine receptor γ gene ($CR\gamma^{-/Y}$) (23), and germ-free (GF) BALB/cA mice (24) have been described previously (13, 15). Recombination activating gene-2 mutant ($RAG\text{-}2^{-/-}$) (25) B/c mice were provided by Dr. S. Koyasu (Keio University School of Medicine, Tokyo, Japan). Ig μ-chain membrane exon-deficient ($\mu m^{-/-}$) mice (26) were a generous gift from Dr. H. Karasuyama (Tokyo Medical and Dental University, School of Medicine, Tokyo, Japan). We obtained transplacentally manipulated PP-deficient mice according to the two methods described elsewhere (8, 9, 27). In brief, timed pregnant B/c mice were injected i.v. with 2 mg of an antagonistic mAb to IL-7R (A7R34) on gestational day 14.5 (27) or 200 μg LTβR-Ig chimeric protein on gestational days 14 and 17 (8). All animal procedures described in this study were performed in according with the guidelines for animal experiments of Keio University School of Medicine.

Abs and lectin

The following mAbs described elsewhere (13–16) were used. For immunohistochemical staining: anti-B220 (RA3-6B2; 2 μg/ml), anti-c-*kit* (ACK-2; 5 μg/ml), anti-CD3 (145-2C11; 5 μg/ml), anti-IL-7R (A7R34; 5 μg/ml) and anti-CD11c (N418; supernatant of the cultured hybridoma) mAbs. Biotinylated peanut agglutinin (PNA; 7.5 μg/ml) (Vector Laboratories) was also used in this study. For flow cytometric analysis: $3–15 \times 10^5$ cells were stained in 50 μl staining medium containing the following mAbs described elsewhere (13–16). FITC-conjugated anti-B220 (RA3-6B2; 5 μg/ml), anti-c-*kit* (ACK-4; 25 μg/ml), and anti-Mac-1 (M1/70; 10 μg/ml) mAbs; and biotinylated anti-IL-7R (A7R34; 30 μg/ml) mAb. FITC-conjugated anti-IgD (11–26c.2a; 20 μg/ml; BD PharMingen, San Diego, CA), anti-IgA (C10-3; 20 μg/ml; BD PharMingen), and anti-T and B cell activation Ag (GL-7; 10 μg/ml; BD PharMingen) mAbs; and biotinylated anti-IgM (R6-60.2; 20 μg/ml, BD PharMingen), anti-B220 (RA3-6B2; 10 μg/ml, BD PharMingen), anti-CD11c (HL3; 10 μg/ml, BD PharMingen), anti-CD5 (53-7.3; 10 μg/ml, BD PharMingen), anti-CD19 (1D3; 10 μg/ml; BD PharMingen), and anti-CD23 (B3B4; 20 μg/ml; BD PharMingen) mAbs as well as biotinylated PNA (0.5 μg/ml; Vector Laboratories) were also used in this study.

Immunohistochemical procedure

Small intestine was longitudinally opened along the mesenteric wall, and then intestine ~10 mm long that had been either kept flat for horizontal section or rolled up for vertical section was embedded in OCT compound (Tissue-Tek; Miles, Elkhalt, IN) at −80°C. The tissue segments were sectioned with a cryostat at 6 μm, and sections were preincubated with Blockace (Dainippon Pharmaceutical, Osaka, Japan) to block nonspecific binding of mAbs. The sections were then incubated with rat or hamster mAb for 30 min at 37°C and rinsed three times with PBS, followed by incubation with biotin-conjugated goat anti-rat IgG Ab (5 μg/ml; Cedarlane Laboratories, Hornby, Ontario, Canada) or with biotin-conjugated goat anti-hamster IgG (5 μg/ml; Cedarlane Laboratories). In staining with biotinylated PNA, the second biotin-conjugated anti-IgG Ab was not used. Subsequently, the sections were washed three times with PBS and then incubated with avidin-biotin peroxidase complexes (Vectastain ABC kit; Vector Laboratories). The histochemical color development was achieved by the Vectastain DAB (3,3′-diaminobenzidine) substrate kit (Vector Laboratories) according to the manufacturer's instructions. Finally, the sections were counterstained with hematoxylin for microscopy. Endogenous peroxidase activity was blocked with 0.3% H_2O_2 and 0.1% NaN_3 in distilled water for 10 min at room temperature. Tissue sections incubated either with isotype-matched normal rat IgG or with nonimmune hamster serum showed only minimal background staining.

In vivo labeling and in situ immunohistochemical visualization of proliferating lymphocytes

Mice were given drinking water containing 1 mg/ml bromodeoxyuridine (BrdU) for 38 h. The small intestines were removed and opened along the mesenteric wall. Then intestines ~10 mm long that had been rolled up were embedded in OCT compound at −80°C. Cryostat tissue sections 9 μm thick that included PP and/or ILF were fixed in 4% paraformaldehyde for 15 min at 4°C, washed three times with PBS, and treated with 2 M HCl for 20 min at 37°C, followed by neutralization with 0.1 M sodium tetraborate. Subsequent immunohistochemical color development using the first anti-BrdU mAb (B44; BD Biosciences, San Jose, CA) and the second biotinylated goat anti-mouse Ig Ab (20 μg/ml; Cappel, Aurora, OH) was performed according to the method described in the preceding section.

Flow cytometry

A single lymphoid cell suspension was prepared, and nucleated cells were counted using a hemocytometer. Resident lymphoid cells in the peritoneal cavity (PEC) were obtained by rinsing PEC with 10 ml ice-cold PBS without Ca^{2+} and Mg^{2+}. ILF cells were isolated by essentially the same technique used for the isolation of CP cells (14–16). In brief, the small intestine was opened longitudinally along the mesenteric wall, and mucus and feces were removed with filter paper. Subsequently, intestine ~10 mm long was pasted on a plastic culture dish. We amputated a needle (18-gauge; inner diameter, 940 μm) at the proximal end of the tapering tip. We then bent the needle in the middle, sharpened its cross-section with the aid of a small electric grinder, i.e., a dental instrument (UA12A; Urawa Kogyo, Saitama, Japan), and finally fitted it on a 1-ml syringe. We located ILF under a transillumination stereomicroscope and isolated a tiny fragment of the small intestine containing one ILF using the needle described above. Lymphoid cells were incubated first with biotinylated mAb and then with streptavidin PE (BD Biosciences) and FITC-conjugated second mAb. Stained cells were suspended in staining medium (Hanks' solution without phenol red, 0.02% NaN_3, and 2% heat-inactivated FBS) containing 0.5 μg/ml propidium iodide (PI) and analyzed using FACScan with CellQuest software (BD Biosciences). Dead cells were excluded by PI gating. Lymphoid cells were incubated with anti-FcγRII/III mAb (2.4G2; 10 μg/ml; BD PharMingen) before staining to block nonspecific binding of labeled mAbs to FcR.

Electron microscopy

Under anesthesia with sodium pentobarbital, B/c mice were perfused transcardially with Ringer's solution and subsequently with a mixture of 2.5% glutaraldehyde and 0.5% paraformaldehyde buffered at pH 7.3 with 0.1 M cacodylate. The small intestine was excised and immersed overnight in the same fixative. After fixation, ILF on the antimesenteric wall were cut out with iridectomy scissors under a dissecting microscope, rinsed in 0.1 M cacodylate buffer (pH 7.3), and postfixed with 1% OsO_4 buffered with cacodylate (0.1 M, pH 7.2) for 2 h. For scanning electron microscopy, the specimens were then dehydrated through a graded series of ethanol, transferred to isoamyl acetate, and critical-point dried with liquid CO_2. The dried specimens were coated with osmium in a plasma osmium coater (Nippon Laser and Electronics Lab, Nagoya, Japan), and examined in a Hitachi H-4500 scanning electron microscope (Hitachi, Tokyo, Japan) at an acceleration voltage of 10 kV. For transmission electron microscopy, the osmicated tissue pieces were dehydrated through a series of ethanol and embedded in Epon 812. Ultrathin sections were examined in a Hitachi H-7100 transmission electron microscope (Hitachi) after double staining with uranyl acetate and lead citrate.

Results

From 100 to 200 lymphoid clusters filled with B220$^+$ cells are distributed throughout the antimesenteric mucosa of the mouse small intestine

During the course of our study on CP (13–16), we noticed the presence of tiny and macroscopically invisible lymphoid clusters filled with B220$^+$ cells in the mouse small intestine, although they are far less frequent but much larger than CP. Recently, we (8) verified that PP are not necessarily obligate GALT for the induction of Ag-specific intestinal IgA and serum IgG Ab responses to an orally administered protein Ag. With these observations in mind, we aimed at investigating the cluster filled with B220$^+$ cells (we use hereafter the term ILF for these B cell aggregations; see below) in detail.

ILF were located in tandem on the antimesenteric wall down from duodenum to ileum in B/c (Fig. 1*A, left*) and B6 (data not shown) mice, whereas CP filled with c-*kit*$^+$ cells were interspersed throughout the mucosa (Fig. 1*A, middle*). We also confirmed antimesenteric localization of multiple ILF in the small intestines of DBA/2J/Jcl and C3H/HeN/Jcl mice (data not shown). ILF were smaller than B cell-enriched follicular units of PP and lacked interfollicular PP regions that contained mainly T cells (Fig. 1*B*). Absolute numbers of ILF in the small bowels of 8- to 20-wk-old adult B/c and B6 mice were 150–200 and 100–150, respectively, and neonatal intestines from these mice lacked ILF. In B/c mice, ILF were not detected at 4 days after birth but became detectable without exception (preferentially in the duodenal and proximal jejunal mucosa) at the 7th postnatal day, the day when CP were first detected in these mice. Postnatal development of ILF in B/c mice is shown in Fig. 2*A*. We also evaluated the frequency DNA replicating cells in ILF and verified that the net accumulation of BrdU-incorporated DNA-replicating cells in ILF was comparable with that in PP (Fig. 2*B*). We (13) have previously reported that CP can be first detected at 14–17 days after birth in the small intestine of B6 mice. However, ILF in B6 intestine remained unidentifiable until day 25 of postnatal life. Thus, although these observations confirm the difference in the time course of postnatal formation of ILF and CP between B/c and B6 animals, histogenetic events behind this difference remain to be explored.

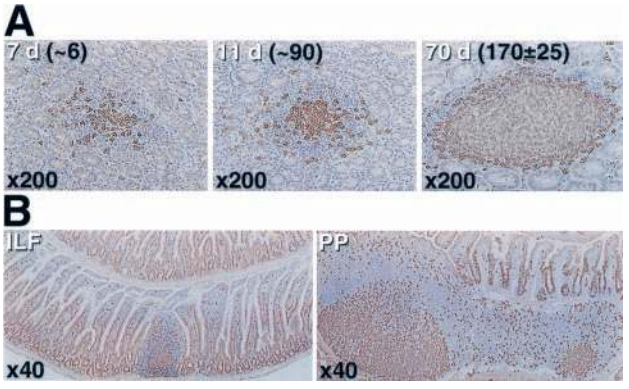

FIGURE 2. Postnatal organogenesis of ILF and immunohistochemical visualization of DNA-replicating cells in ILF. *A,* ILF in B/c mice were not detected at day 4 after birth but became detectable without exception at the 7th postnatal day. The numbers of ILF per small intestine from three to five mice are shown. *B,* BrdU-incorporated lymphocytes in ILF and PP from adult B/c mice. Cells that reside in GC of ILF and PP exhibit massive proliferation.

ILF and CP are distinct organized GALT of the mouse small intestine

CP are located mostly in the crypt LP and are not subdivided into specific areas based on their cellular composition (13). We found in the present study that ILF were larger than CP (Fig. 1*A*) and appeared to occupy both the crypt and villous LP (Fig. 1*B*). To compare more precisely the anatomical and cellular features of ILF with those of CP, immunohistochemical analysis was conducted using five representative mAbs that were reactive with B cells

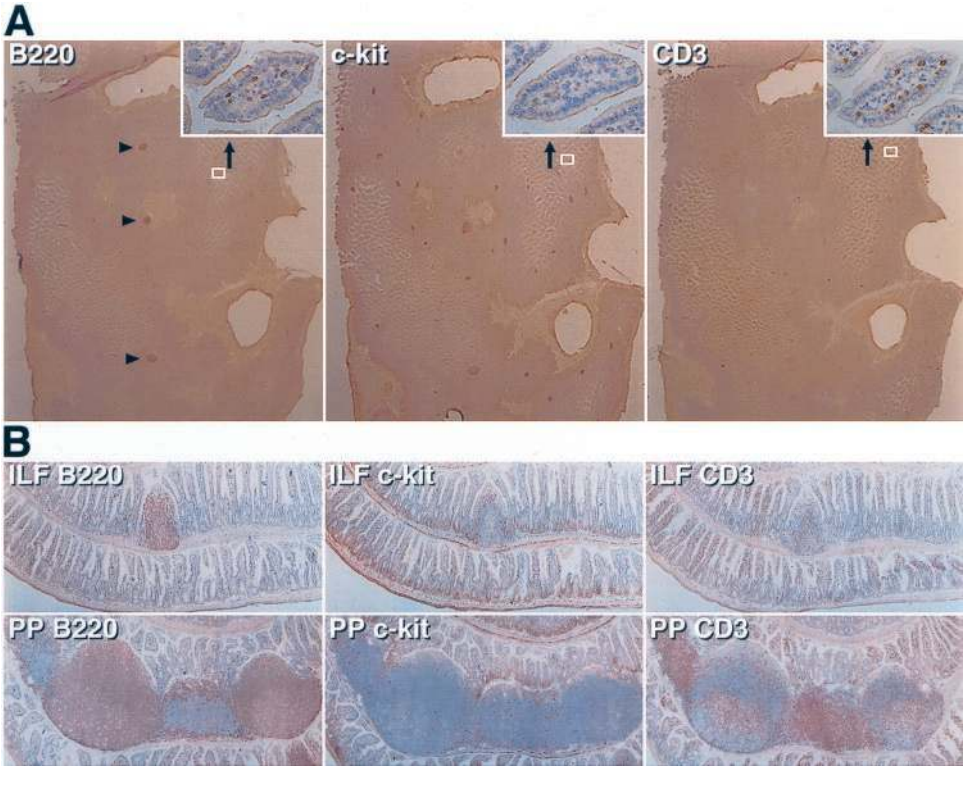

FIGURE 1. Immunohistochemical visualization of B220$^+$ (ILF) and c-*kit*$^+$ (CP) cell aggregations and PP in the small intestine of B/c mice. We examined the entire small intestine, and representative jejunal pictures are shown. *A*, Consecutive tissue sections were stained with anti-B220 (*left*), anti-c-*kit* (*middle*) and anti-CD3 (*right*) mAb, respectively (×15). Three ILF are aligned along the antimesenteric wall of the mucosa (arrowheads) and that numerous tiny CP are interspersed throughout the mucosa. Magnified views (×400) of the rectangular areas are also presented in at the *upper right* (arrows). *B*, Immunohistochemical analysis of ILF and PP on the consecutive vertical tissue sections of the small intestine (×80). Note that ILF lack T (CD3$^+$) cell-enriched interfollicular regions that are the well-acknowledged component of PP (*lower right*).

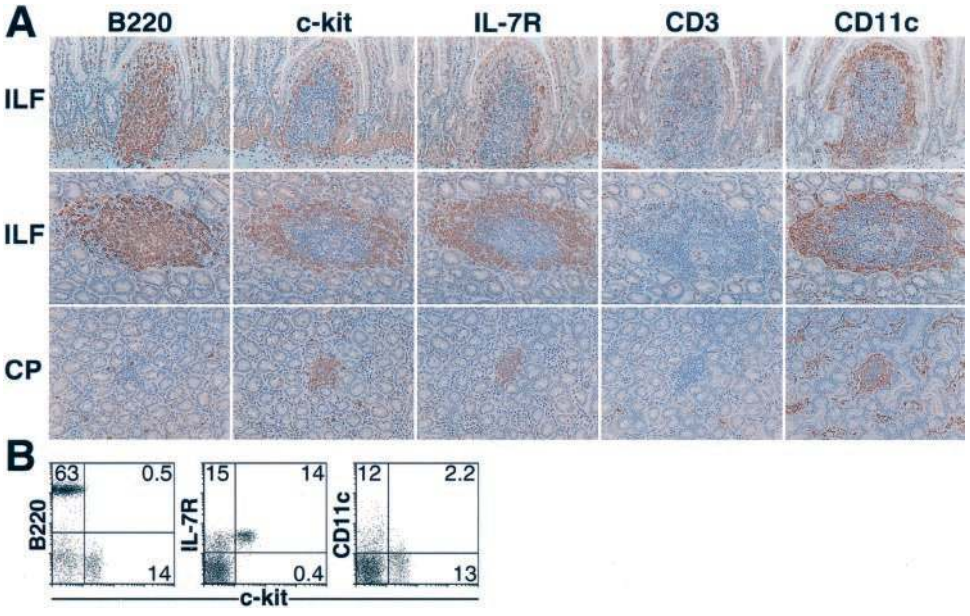

FIGURE 3. Immunohistochemical characterization of cells in ILF and CP and flow cytometric analysis of cells that sojourn in ILF. *A*, Cells expressing B220, c-*kit*, IL-7R, CD3, and CD11c molecules on the consecutive tissue sections were examined by immunohistochemistry (×200). Vertical (*top*) and horizontal (*middle*) profiles of ILF and horizontal (*bottom*) profiles of CP. As also depicted in Fig. 1*B*, villi housing ILF are thicker and shorter in the vertical section than surrounding classical villi and are distinguished by containing LP that are replaced by a major population of cells expressing B220. CP are void of not only $CD3^+$ cells but also $B220^+$ cells. *B*, Two-color flow cytometric analysis of cells isolated from ILF. Note that c-kit^+IL-$7R^+$ cells are neither $B220^+$ nor $CD11c^+$. The percentage of positive cells in the corresponding quadrants is shown.

(B220), mature T cells (CD3), lymphohemopoietic precursor cells (c-kit and IL-7R) or dendritic stromal cells (CD11c), and the results are presented in Fig. 3*A*. On the basis of vertical profile, villi containing ILF were thicker (barrel-shaped) and shorter than surrounding villi not containing ILF (Figs. 1*B* and 3*A*, *top*). The collection of B cells that resided the central region of ILF was surrounded by the layer of cells expressing c-*kit* and IL-7R molecules, and a considerable number of dendritic $CD11c^+$ cells were distributed in the peripheral region of ILF (Fig. 3*A, top* and *middle*). Flow cytometric analysis of lymphoid cells isolated from ILF confirmed that the $B220^+$, c-kit^+IL-$7R^+$, and $CD11c^+$ cells constituted three discrete nonoverlapping populations (Fig. 3*B*). A small number of $CD3^+$ T cells was also interspersed within the ILF (Figs. 1*B* and 3*A*). Finally, transverse profiles clearly showed that the average diameter of ILF was longer by a factor of 2–5 compared with that of CP, and, as verified previously (13), neither B cells nor mature T cells were localized in CP (Fig. 3*A, bottom*). These findings suggest that ILF and CP constitute two distinct organized GALT in the mouse small intestine.

ILF include germinal center (GC) and epithelia overlying ILF contain microfold (M) cells

During the course of immunohistochemical study on ILF, we realized that the lymphocytes compartmentalized in a core area of the $B220^+$ cell aggregations are proliferating vigorously (Fig. 2*B*) and appear to include B blasts. In lymphoid follicles, B cells at active immune responses can be identified by their distinctive ability to bind PNA (28) and the mAb GL-7 (29, 30) and undergo clonal expansion in forming GC. In this context, we examined whether or not these putative B blasts were capable of binding PNA and found that, in addition to the well-known GC formation in PP (Fig. 4*A, bottom*), PNA^+ cell clusters, namely GC, were present in the central area of the $B220^+$ cell aggregations (Fig. 4*A, upper left* and *middle*). In contrast, CP were void of such PNA-reactive cells (Fig. 4*A, upper right*). Among cells isolated from ILF, PP, MLN, and spleen of nonimmunized normal B/c mice examined, a substantial fraction of $B220^+$ ILF cells was PNA^+ and/or $GL\text{-}7^+$, and a large fraction of $B220^+$ PP cells was PNA^+ and/or $GL\text{-}7^+$, whereas only a minimal fraction of $B220^+$ MLN cells and $B220^+$ splenic cells displayed PNA^+ and/or $GL\text{-}7^+$ phenotypes (Fig. 4*B*), indicating the persistent GC formation in ILF and PP due to the constant antigenic challenge from the gastrointestinal tract.

Follicle-associated epithelium not only has typical columnar enterocytes but also contains M cells that deliver various luminal Ags

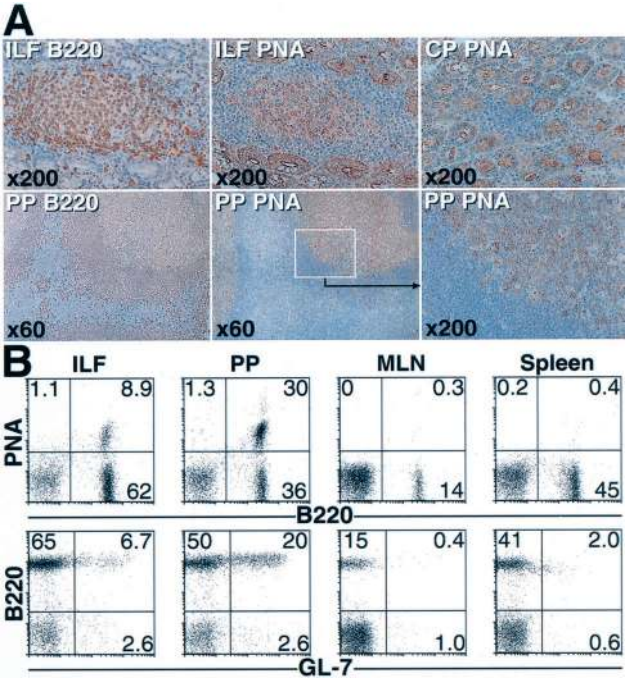

FIGURE 4. Immunohistochemical and flow cytometric verification of GC formation in ILF. *A*, A cluster of PNA binding (PNA^+) cells (*upper middle*) is compartmentalized in the central region of $B220^+$ cell aggregation (*upper left*), namely, ILF, and CP are void of such PNA^+ cells (*upper right*). In the lower panels, one well-established cluster of PNA^+ PP cells (GC) (*middle*) and the surrounding corona of $B220^+$ B cells (*left*) are shown as a positive control. *B*, Two-color flow cytometric analysis was performed on cells isolated from ILF, PP, MLN, and spleen. Although the population size of PNA^+ and/or $GL\text{-}7^+$ subsets of ILF compartment is smaller than that of PP, a significant fraction of cells in ILF expresses ligands for PNA and GL-7, indicating the presence of GC B cells in ILF. In contrast, few if any cells from MLN and spleen are PNA^+ and/or $GL\text{-}7^+$. The percentage of positive cells in the corresponding quadrants is shown.

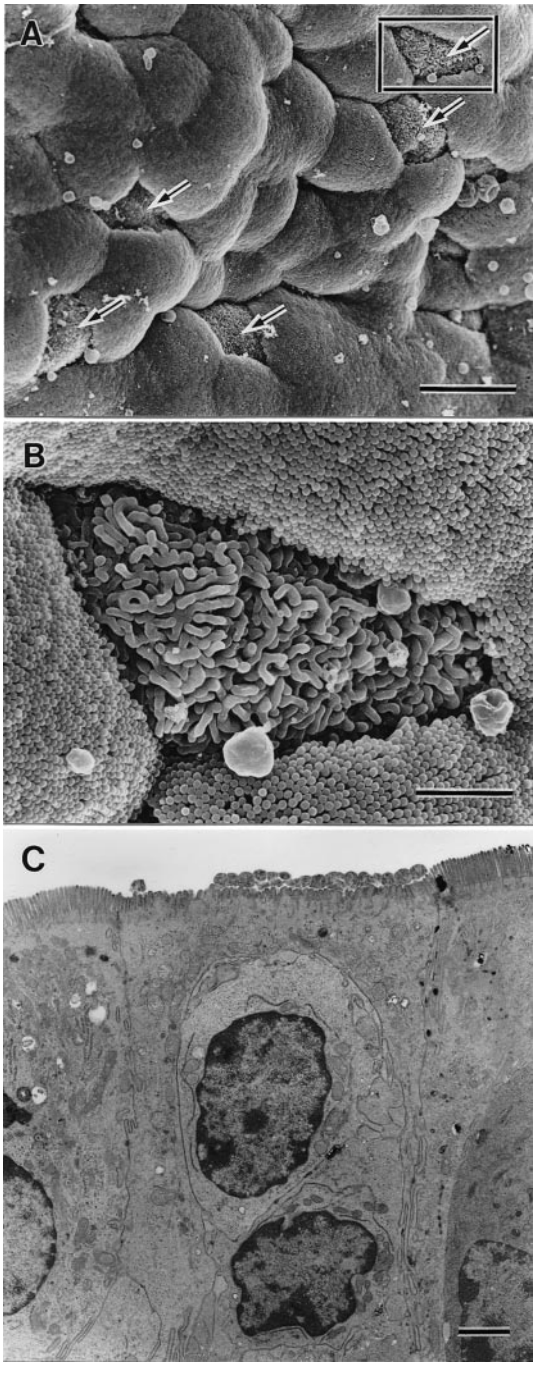

FIGURE 5. Electron microscopic analysis of the epithelium adjacent to ILF. *A*, Scanning electron micrograph of epithelium overlying ILF which shows the presence of five M cells (arrows). Bar, 10 μm. *B*, Magnified view of the *inset* in Fig. 4*A*. The M cell in the center is surrounded by absorptive enterocytes that possess numerous closely packed regular microvilli on their apices. Note the short, wide and irregular microvilli of the M cell. Bar, 2 μm. *C*, Transmission electron micrograph of M cell in the epithelium overlying ILF. Microvilli of the M cell (*center*) are shorter, thicker, and less abundant than those of surrounding absorptive enterocytes, and this M cell enfolds two lymphoid cells. Bar, 2 μm.

to GALT (31). Electron microscopy of epithelia overlying the $B220^+$ cell aggregations revealed that the epithelia contained M cells (Figs. 5, *A* and *B*), and these M cells were found to enfold lymphoid cells in their central hollow (Fig. 5*C*). Thus, taking all of the above findings collectively, these $B220^+$ cell aggregations are the first identification of ILF in the mouse small intestine.

Flow cytometric analysis of B cells that reside in ILF

IgA is a predominant Ig which is secreted mainly across mucous membranes, and the LP of intestines contains the largest collection of IgA-producing plasma cells. These plasma cells have been shown to derive either from the conventional Ag-specific IgA-committed B-2 cells in PP (4, 32) or from the B-1 cells (33, 34) that are enriched among B cells compartmentalized in the PEC (35). To determine whether B cells that reside in ILF are similar or dissimilar to those of PP, flow cytometric analysis was conducted (Fig. 6). Both ILF and PP harbored a large population of IgM^+ B cells and also a significant population of IgA^+ B cells, whereas MLN contained few IgA^+ B cells (Fig. 6, *top*). B cells isolated from ILF, PP, and MLN appeared to be $IgM^{low}IgD^{high}$ as compared with those recovered from PEC, the majority of which displayed $IgM^{high}IgD^{low}$ phenotype (Fig. 6, *middle*). In contrast to the fact that two-thirds of $B220^+$ PEC cells expressed CD5 (Fig. 6, *bottom*) and Mac-1 (data not shown) molecules, such $B220^+CD5^+$ cells (Fig. 6, *bottom*) and $B220^+$Mac-1^+ cells (data not shown) were minimal in ILF, PP, and MLN compartments. Moreover, almost all $B220^+$ cells from ILF and PP were $CD19^+$, and a large fraction of them were $CD23^+$, whereas $B220^+$ cells from PEC remained $CD23^-$ (data not shown). Because mucosal B cells have been classified into B-1 and B-2 cells based on the differential expression of B220, IgM, IgD, CD5, Mac-1, and CD23 molecules (34, 36), the present findings suggest that ILF are inductive sites for initiation of IgA-committed B-2 cell responses in the gastrointestinal tract.

ILF in GF, various mutant and transplacentally manipulated PP-deficient mice

Immunohistochemical analysis was conducted to characterize ILF of GF and various mutant mice (Fig. 7). We evaluated the effects of microbial and thymic deprivations in GF (Fig. 7*B*) and *nu/nu* (Fig. 7*C*) mice, respectively, on the development of ILF and found that the cellularity of ILF remained the same in both animals. However, c-kit^+ cells outnumbered $B220^+$ cells (Fig. 7, *B* and *C*) and the formation of GC was hardly detectable (data not shown) under these conditions. The cellular mass of ILF was also not significantly altered in the *RAG-*$2^{-/-}$ (Fig. 7*D*), TCR-$\beta^{-/-}$ (Fig.

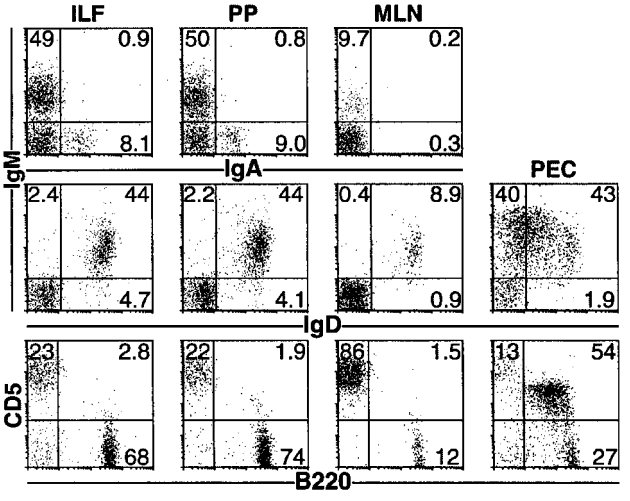

FIGURE 6. B cells that reside in ILF are B-2 rather than B-1 B cells and are phenotypically similar to those that reside in PP but dissimilar to those recovered from PEC, a large fraction of which displays the phenotype of B-1 B cells. Two-color flow cytometric analysis was performed on cells isolated from ILF, PP, MLN, and PEC. The percentage of positive cells in the corresponding quadrants is shown.

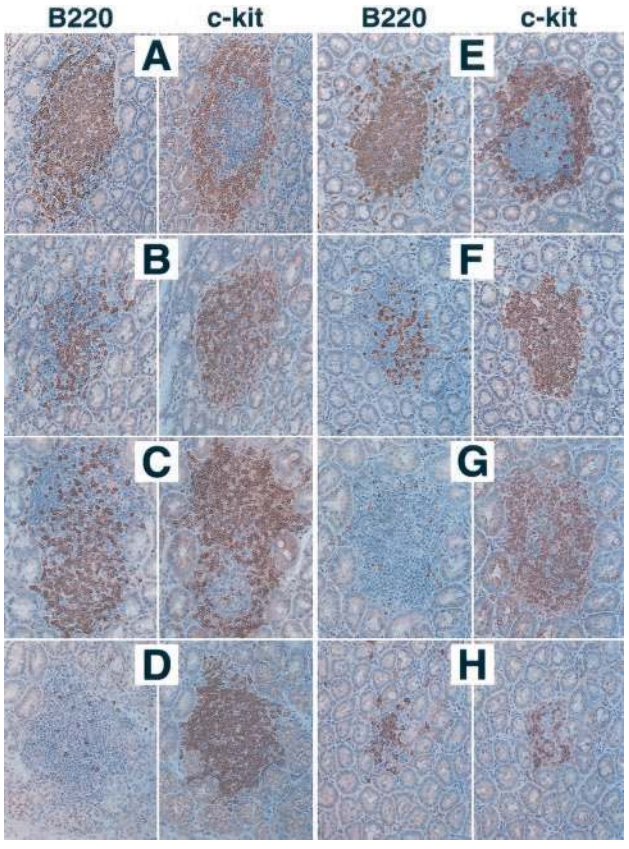

FIGURE 7. Representative immunohistochemical visualization of B220$^+$ and c-*kit*$^+$ lymphocytes in jejunal ILF from wild-type B/c (*A*), GF (*B*), *nu/nu* (*C*), *RAG-2*$^{-/-}$ (*D*), wild-type B6 (*E*), TCR-$\beta^{-/-}$ (*F*), $\mu m^{-/-}$ (*G*) and IL-7R$\alpha^{-/-}$ (*H*) mice. Mice *A–D* have a genetic background of the B/c strain and mice *E–H* have a genetic background of the B6 strain. Original magnification, ×400.

7*F*), and $\mu m^{-/-}$ (Fig. 7*G*) conditions as compared with those of wild-type ILF from B/c (Fig. 7*A*) and B6 (Fig. 7*E*) mice, whereas the difference in cellular composition was striking. Thus, the population size of B220$^+$ cells was reduced drastically in TCR-$\beta^{-/-}$ ILF (Fig. 7*F*), and few, if any, B220$^+$ cells were detected in *RAG-2*$^{-/-}$ (Fig. 7*D*) and $\mu m^{-/-}$ (Fig. 7G) ILF. In these three mutant ILF, especially in *RAG-2*$^{-/-}$ and $\mu m^{-/-}$ ILF, c-*kit*$^+$ cells replaced B220$^+$ cells as the predominant population. As far as the lymphoid residents of PP are concerned, c-*kit*$^+$ cells occupied interfollicular T cell regions in TCR-$\beta^{-/-}$ PP, follicular B cell regions in $\mu m^{-/-}$ PP and entire T and B cell regions in *RAG-2*$^{-/-}$ PP (data not shown). As in the histogenesis of CP (13, 15), sharply emaciated ILF were detected in IL-7R$\alpha^{-/-}$ mice (Fig. 7*H*).

To determine whether ILF are newly identified murine GALT distinct in terms of organogenesis from PP, we determined the number of ILF in various animals, and the results obtained are presented in Table I. Absolute numbers of ILF were not significantly altered in GF, *nu/nu*, *RAG-2*$^{-/-}$, and TCR-$\beta^{-/-}$ mice as compared with those of the corresponding wild-type ILF, whereas absolute numbers of ILF in $\mu m^{-/-}$ mice were about one-half of those in B6 mice. Finally, a drastically reduced number of ILF was detected in IL-7R$\alpha^{-/-}$ PP^{null} mice. It has been reported that PP are absent from the small intestines of LT$\alpha^{-/-}$ (20) and *aly/aly* (19) mutant mice. In this context, we addressed whether these mutations affect the development of ILF and found that histogenesis of ILF was also completely blocked. In these mutant conditions, however, histogenesis of CP and intestinal development of intraepithelial T cells (IEL) that derive from c-*kit*$^+$ CP cells (14, 16) remained intact. It has recently been verified that not only PP but also CP are absent from *CR*$\gamma^{-/Y}$ mice. We found that ILF were hardly detectable in the intestinal LP of these *CR*$\gamma^{-/Y}$ mice. We also determined the development of ILF in the transplacentally manipulated PP^{null} mice because previous studies have shown that exposure to anti-IL-7R mAb (27) as well as exposure to LTβR-Ig chimeric protein (8, 9) during gestation disrupted PP but not MLN formation. As a result, it was confirmed that the offspring from these mothers lacked PP but possessed well-developed ILF (Table I) and CP (data not shown). In conclusion, ILF are not identical with PP or with CP with respect to their histogenesis and lymphocyte composition, and it is quite intriguing that they are aligned along the antimesenteric wall of the mouse small intestine.

Table I. *Number of ILF and PP in the small intestine of various mice*[a]

	Mice (*n*)	ILF	PP
A.	B/c (11)	178 ± 31	9.0 ± 1.8
	GF (4)	157 ± 15	9.5 ± 1.3[b]
	nu/nu (4)	152 ± 12	8.5 ± 3.1
	RAG-2$^{-/-}$ (4)	129 ± 20	8.5 ± 1.3[c]
	Anti-IL-7R[d] (5)	168 ± 25	UD
	LTβR-Ig[e] (3)	174 ± 16	UD
B.	B6 (6)	143 ± 16	8.0 ± 1.8
	TCR-$\beta^{-/-}$ (4)	134 ± 17	7.8 ± 1.0
	$\mu m^{-/-}$ (4)	70 ± 18	6.5 ± 1.3[b]
	IL-7R$\alpha^{-/-}$ (4)	36 ± 6[c]	UD
	LT$\alpha^{-/-}$ (4)	UD	UD
	aly/aly (5)	UD	UD
	CR$\gamma^{-/Y}$ (6)	UD	UD

[a] Immunohistochemical verification of the small intestine in various mice carrying B/c (A) or B6 (B) genetic background. The numbers of ILF and PP per mouse ± SD are presented. UD, undetectable.
[b] Significantly attenuated in size.
[c] Sharply attenuated in size.
[d] Mother B/c mice were injected i.v. with 2 mg anti-IL-7R mAb (A7R34) on gestational day 14.5.
[e] Mother B/c mice were injected i.v. with 200 μg LTβR-Ig chimeric protein on gestational days 14 and 17.

Discussion

To our knowledge, we are the first to identify ~100–200 lymphoid aggregations that satisfied the structural and cellular requirements of ILF in mouse small intestine. Remarkably, they were aligned at roughly regular intervals along the antimesenteric wall of the small bowel (Fig. 1*A, left*). In addition to ~10 aggregated lymphoid follicles (37), we also verified that ~50 ILF were interspersed throughout the large intestinal mucosa of B/c mice (data not shown). We do not know why they have not been described to date, but we believe the existence of CP and ILF in the murine intestinal mucosa has not been previously evaluated and reported simply because they are very small and constitute only a thinly scattered population. Immunohistochemical examination revealed that villi housing ILF are thicker and shorter in a longitudinal section than surrounding classical villi, and they are distinguished by containing a LP that is replaced by closely packed lymphocytes (Figs. 1*B* and 3*A*). In this regard, ILF are structures that resemble most closely LFV of the rat small intestine (17), although their lymphoid residents are markedly different from those of rat LFV, a large fraction of which displays an immature phenotype (17). Thus, in agreement with the properties of ILF described in other mammals (7, 11, 12), it is evident that mouse ILF identified in the present study are similar to the follicular units that compose PP.

As far as organogenesis is concerned, however, the difference between ILF and PP is a matter of considerable interest. First, ILF

are not detectable until day 4 (B/c mice) or day 25 (B6 mice) of postnatal life, whereas PP are already microscopically well developed by just before birth in both strains of mouse (Ref. 27 and data not shown). Second, in utero treatment with anti-IL-7R mAb or LTβR-Ig chimeric protein abrogates the development of PP, leaving that of ILF unaffected. Third, IL-7R$\alpha^{-/-}$ mice lack PP, whereas they possess ILF-like lymphoid aggregations although they are atrophied markedly in both average size (Fig. 7*H*) and numbers. Because the present findings (Figs. 4 and 6) support the notion that ILF are also the inductive sites for intestinal IgA Ab responses to a variety of luminal Ags, the biological significance of the difference in ILF and PP formation is most likely to be failsafe and/or mutually compensatory systems for the maintenance of intestinal immune surveillance. In mice, organogenesis of 6 to 12 PP involves at least 3 distinct steps in the late embryonic stage (27). Exposure of day 14.5 to 15.5 fetuses, namely, the first step, to anti-IL-7R mAb results in the generation of PP^{null} but otherwise normal mice (Ref. 27 and Table I), indicating that there exists a short and critical time window during the initial step of PP formation. In contrast, organogenesis of ILF commences in early postnatal life and thereafter increases gradually in numbers and average size (Fig. 2*A*). In the context of these findings and given that PP have evolved earlier than ILF, it is conceivable that the development of ILF in the mouse small intestine is a failsafe system. Conversely, if the ILF evolved earlier than PP, the development of PP is regarded as a complementary system to the lack of ILF during early infantile life. In any case, exploration of these possibilities is certainly an important goal for future experiments.

Not only PP but also ILF are absent from LT$\alpha^{-/-}$ and *aly/aly* mice, whereas CP and their IEL descendants are present in these mutant animals (14, 16, 38) and, in contrast to antimesenteric distribution of PP and ILF, CP are situated randomly around the circumference of the intestinal wall (Fig. 1*A*). Intriguingly, however, organogeneses of ILF and CP commence at the same postnatal age in B/c mice, although that of PP is completed just before birth. Because it has recently been demonstrated that LTα1β2 receptor (LTβR) signaling is crucial for the first step of PP formation (27) and that LTβR-mediated activation of NF-κB-inducing kinase is selectively cancelled in the *aly* mutation (39), it is evident that the signal passing through LTβR at antimesenteric organizing centers is indispensable for the formation of both PP and ILF anlagen. In sharp contrast, neither LTα1β2 nor the positional signals that emanate solely from antimesenteric mucosa are essential for the formation of CP anlagen. Also, the lymphoid follicles in the cecum (cecal patch), which are surprisingly quite intact in IL-7R$\alpha^{-/-}$ mice (27), are absent in LT$\alpha^{-/-}$ and *aly/aly* mice (H. Yoshida, unpublished observations). All in all, LT$\alpha^{-/-}$ and *aly/aly* mice lack PP, ILF, and cecal patch but possess well-developed CP, IL-7R$\alpha^{-/-}$ mice lack PP but possess normal cecal patch and conspicuously atrophied ILF and CP, and *CR*$\gamma^{-/Y}$ mice are void of PP, ILF, and CP. Taking these observations at face value, there exists remarkable complexity in the organogenetic mechanism of different GALT, and much remains to be learned about molecular level of cellular events underlying the formation of these organized GALT before we elucidate the biological significance of this complexity.

In addition to PP and CP, lymphoid aggregations analogous to ILF of wild-type mice are present in *nu/nu*, *RAG-2*$^{-/-}$, and μm$^{-/-}$ mice, indicating that organogenesis of ILF anlagen is dependent neither on thymus-derived lymphocytes nor on the expression of Ag receptor genes on T and B cells. However, ILF detected in *RAG-2*$^{-/-}$ and μm$^{-/-}$ mice are phenotypically abnormal because most lymphoid cells express c-*kit* but not B220 molecules (Figs. 7, *D* and *G*). These results not only indicate that the organogenesis of ILF proceeds through at least several histologically distinct steps but also suggest that B lineage-committed cells and/or mature B cells immigrate from outside into ILF during the latter stage of ILF formation. In conclusion, the current studies identified and characterized ILF in mouse small intestine and illuminated the various facets of their postnatal development. We consider that our findings are of considerable importance because researchers exploring the distinctive features of intestinal immune responses to luminal Ags such as the regulation of mucosal IgA Ab responses and induction of oral tolerance in the gastrointestinal tract, and the role of PP in these processes have been performing their experiments using various manipulated laboratory mice, including the mice that lack PP but possess ILF.

Acknowledgments

We thank Drs. S. Koyasu and H. Karasuyama for providing RAG-2$^{-/-}$ BALB/c mice and μm$^{-/-}$ mice, respectively, and K. Ishimaru and Y. Harashima for their technical assistance.

References

1. Neutra, M. R., P. Michetti, and J.-P. Kraehenbuhl. 1994. Secretory immunoglobulin A: induction, biogenesis, and function. In *Physiology of the Gastrointestinal Tract,* 3rd ed., Vol. 2. L. R. Johnson, ed. Raven Press, New York, p. 685.
2. Russell, M. W., M. Kilian, and M. E. Lamm. 1999. Biological activities of IgA. In *Mucosal Immunology,* 2nd ed. P. L. Ogra, J. Mestecky, M. E. Lamm, W. Strober, J. Bienestock, and J. R. McGhee, eds. Academic Press, San Diego, p. 225.
3. Macpherson, A. J., D. Gatto, E. Sainsbury, G. R. Harriman, H. Hengartner, and R. M. Zinkernagel. 2000. A primitive T cell-independent mechanism of intestinal mucosal IgA responses to commensal bacteria. *Science 288:2222.*
4. Craig, S. W., and J. J. Cebra. 1971. Peyer's patches: an enriched source of precursors for IgA-producing immunocytes in the rabbit. *J. Exp. Med. 134:188.*
5. McIntyre, T. M., and W. Strober. 1999. Gut-associated lymphoid tissue: regulation of IgA B-cell development. In *Mucosal Immunology.* R. L. Ogra, J. Mestecky, M. E. Lamm, W. Strober, J. Bienenstock, and J. R. McGhee, eds. Academic Press, San Diego, p. 319.
6. Heatley, R. V., J. M. Stark, P. Horsewood, E. Bandouvas, F. Cole, and J. Bienenstock. 1981. The effects of surgical removal of Peyer's patches in the rat on systemic antibody responses to intestinal antigen. *Immunology 44:543.*
7. Keren, D. F., P. S. Holt, H. H. Collins, P. Gemski, and S. B. Formal. 1978. The role of Peyer's patches in the local immune response of rabbit ileum to live bacteria. *J. Immunol. 120:1892.*
8. Yamamoto, M., P. Rennert, J. R. McGhee, M.-N. Kweon, S. Yamamoto, T. Dohi, S. Otake, H. Bluethmann, K. Fujihashi, and H. Kiyono. 2000. Alternate mucosal immune system: organized Peyer's patches are not required for IgA responses in the gastrointestinal tract. *J. Immunol. 164:5184.*
9. Rennert, P. D., J. L. Browning, and P. S. Hochman. 1997. Selective disruption of lymphotoxin ligands reveals a novel set of mucosal lymph nodes and unique effects on lymph node cellular organization. *Int. Immunol. 9:1627.*
10. Eugster, H.-P., M. Muller, U. Karrer, B. D. Car, B. Schnyder, V. M. Eng, G. Woerly, M. Le Hir, F. di Padova, M. Aguet, et al. 1996. Multiple immune abnormalities in tumor necrosis factor and lymphotoxin-α double-deficient mice. *Int. Immunol. 8:23.*
11. Moghaddami, M., A. Cummins, and G. Mayrhofer. 1998. Lymphocyte-filled villi: comparison with other lymphoid aggregations in the mucosa of the human small intestine. *Gastroenterology 115:1414.*
12. Rosner, A. J., and D. F. Keren. 1984. Demonstration of M cells in the specialized follicle-associated epithelium overlying isolated lymphoid follicles in the gut. *J. Leukocyte Biol. 35:397.*
13. Kanamori, Y., K. Ishimaru, M. Nanno, K. Maki, K. Ikuta, H. Nariuchi, and H. Ishikawa. 1996. Identification of novel lymphoid tissues in murine intestinal mucosa where clusters of c-*kit*$^+$IL-7R$^+$Thy-1$^+$ lympho-hemopoietic progenitors develop. *J. Exp. Med. 184:1449.*
14. Saito, H., Y. Kanamori, T. Takemori, H. Nariuchi, E. Kubota, H. Takahashi-Iwanaga, T. Iwanaga, and H. Ishikawa. 1998. Generation of intestinal T cells from progenitors residing in gut cryptopatches. *Science 280:275.*
15. Oida, T., K. Suzuki, M. Nanno, Y. Kanamori, H. Saito, E. Kubota, S. Kato, M. Itoh, S. Kaminogawa, and H. Ishikawa. 2000. Role of gut cryptopatches in early extrathymic maturation of intestinal intraepithelial T cells. *J. Immunol. 164:3616.*
16. Suzuki, K., T. Oida, H. Hamada, O. Hitotsumatsu, M. Watanabe, T. Hibi, H. Yamamoto, E. Kubota, S. Kaminogawa, and H. Ishikawa. 2000. Gut cryptopatches: direct evidence of extrathymic anatomical sites for intestinal T lymphopoiesis. *Immunity 13:691.*
17. Mayrhofer, G., M. Moghaddami, and C. Murphy. 1999. Lymphocyte-filled villi (LFV): non-classical organized lymphoid tissues in the mucosa of the small intestine. *Mucosal Immunol. Update 7:9.*
18. Lefrancois, L., and L. Puddington. 1998. Anatomy of T-cell development in the intestine. *Gastroenterology 115:1588.*
19. Miyawaki, S., Y. Nakamura, H. Suzuka, M. Koba, R. Yasumizu, S. Ikehara, and Y. Shibata. 1994. A new mutation, *aly*, that induces a generalized lack of lymph nodes accompanied by immunodeficiency in mice. *Eur. J. Immunol. 24:429.*

20. De Togni, P., J. Goellner, N. H. Ruddle, P. R. Streeter, A. Fick, S. Mariathasan, S. C. Smith, R. Carlson, L. P. Shornick, J. Strauss-Schoenberger, J. H. Russell, R. Karr, and D. D. Chaplin. 1994. Abnormal development of peripheral lymphoid organs in mice deficient in lymphotoxin. *Science 264:703.*
21. Maki, K., S. Sunaga, Y. Komagata, Y. Kodaira, A. Mabuchi, H. Karasuyama, K. Yokomuro, J. Miyazaki, and K. Ikuta. 1996. Interleukin 7 receptor-deficient mice lack γδ T cells. *Proc. Natl. Acad. Sci. USA 93:7172.*
22. Mombaerts, P., A. R. Clarke, M. A. Rudnicki, J. Iacomini, S. Itohara, J. J. Lafaille, L. Wang, Y. Ichikawa, R. Jaenisch, M. L. Hooper, and S. Tonegawa. 1992. Mutations in T-cell antigen receptor genes α and β block thymocyte development at different stages. *Nature 360:225.*
23. Ohbo, K., T. Suda, M. Hashiyama, A. Mantani, M. Ikebe, M. Miyakawa, M. Moriyama, M. Nakamura, M. Katsuki, K. Takahashi, K. Yamamura, and K. Sugamura. 1996. Modulation of hematopoiesis in mice with a truncated mutant of the interleukin-2 receptor γ chain. *Blood 87:956.*
24. Kawaguchi, M., M. Nanno, Y. Umesaki, S. Matsumoto, Y. Okada, Z. Cai, T. Shimamura, Y. Matsuoka, M. Ohwaki, and H. Ishikawa. 1993. Cytolytic activity of intestinal intraepithelial lymphocytes in germ-free mice is strain dependent and determined by T cells expressing γδ T-cell antigen receptors. *Proc. Natl. Acad. Sci. USA 90:8591.*
25. Shinkai, Y., G. Rathbun, K. P. Lam, E. M. Oltz, V. Stewart, M. Mendelsohn, J. Charron, M. Datta, F. Young, A. M. Stall, and F. W. Alt. 1992. RAG-2-deficient mice lack mature lymphocytes owing to inability to initiate V(D)J rearrangement. *Cell 68:855.*
26. Kitamura, D., J. Roes, R. Kuhn, and K. Rajewsky. 1991. A B cell-deficient mouse by targeted disruption of the membrane exon of the immunoglobulin μ chain gene. *Nature 350:423.*
27. Yoshida, H., K. Honda, R. Shinkura, S. Adachi, S. Nishikawa, K. Maki, K. Ikuta, and S.-I. Nishikawa. 1999. IL-7 receptor α^+ $CD3^-$ cells in the embryonic intestine induces the organizing center of Peyer's patches. *Int. Immunol. 11:643.*
28. Rose, M. L., M. S. C. Birbeck, V. J. Wallis, J. A. Forrester, and A. J. S. Davies. 1980. Peanut lectin binding properties of germinal centres of mouse lymphoid tissue. *Nature 284:364.*
29. Han, S., B. Zheng, D. G. Schatz, E. Spanopoulou, and G. Kelsoe. 1996. Neoteny in lymphocytes: Rag1 and Rag2 expression in germinal center B cells. *Science 274:2094.*
30. Laky, K., L. Lefrancois, E. G. Lingenheld, H. Ishikawa, J. M. Lewis, S. Olson, K. Suzuki, R. E. Tigelaar, and L. Puddington. 2000. Enterocyte expression of IL-7 induces development of γδ T cells and Peyer's patches. *J. Exp. Med. 191: 1569.*
31. Owen, R. L. 1999. Uptake and transport of intestinal macromolecules and microorganisms by M cells in Peyer's patches—a personal and historical perspective. *Semin. Immunol. 11:157.*
32. Husband, A. J., and J. L. Gowans. 1978. The origin and antigen-dependent distribution of IgA-containing cells in the intestine. *J. Exp. Med. 148:1146.*
33. Hayakawa, K., R. R. Hardy, D. R. Parks, and L. A. Herzenberg. 1983. The "Ly-1 B" cell subpopulation in normal immunodefective, and autoimmune mice. *J. Exp. Med. 157:202.*
34. Fagarasan, S., and T. Honjo. 2000. T-independent immune response: New aspects of B cell biology. *Science 290:89.*
35. Kroese, F. G. M., E. C. Butcher, A. M. Stall, P. A. Lalor, S. Adams, and L. A. Herzenberg. 1989. Many of the IgA producing plasma cells in murine gut are derived from self-replenishing precursors in the peritoneal cavity. *Int. Immunol. 1:75.*
36. Hardy, R. R., and K. Hayakawa. 1994. CD5 B cells, a fetal B cell lineage. *Adv. Immunol. 55:297.*
37. Owen, R. L., A. J. Piazza, and T. H. Ermak. 1991. Ultrastructural and cytoarchitectural features of lymphoreticular organs in the colon and rectum of adult BALB/c mice. *Am. J. Anat. 190:10.*
38. Nanno, M., S. Matsumoto, R. Koike, M. Miyasaka, M. Kawaguchi, T. Masuda, S. Miyawaki, Z. Cai, T. Shimamura, Y. Fujiura, and H. Ishikawa. 1994. Development of intestinal intraepithelial T lymphocytes is independent of Peyer's patches and lymph nodes in *aly* mutant mice. *J. Immunol. 153:2014.*
39. Shinkura, R., K. Kitada, F. Matsuda, K. Tashiro, K. Ikuta, M. Suzuki, K. Kogishi, T. Serikawa, and T. Honjo. 1999. Alymphoplasia is caused by a point mutation in the mouse gene encoding NF-κB-inducing kinase. *Nat. Genet. 22:74.*